Configuration interaction and Raman redistribution in perturbed Ba Rydberg states

M. L. Bajema, R. van Leeuwen, E. Murgu, and T. F. Gallagher
Department of Physics, University of Virginia, Charlottesville, Virginia 22901
(Received 30 July 1999; published 14 January 2000)

We have experimentally observed the time dependence of the population oscillation between a doubly excited state and singly excited Rydberg states subsequent to excitation by a short laser pulse. Specifically, we have examined the case in which the configuration interaction between a doubly excited state and a singly excited Rydberg series is weak. The data are quantitatively reproduced using a quantum defect theory calculation, and we contrast simple classical pictures of the population oscillation for weak and strong configuration interaction. We also observe significant, and unexpected, Raman redistribution by the final laser pulse, and we are able to demonstrate that it occurs primarily by Raman transitions via a lower state, not via the continuum.

PACS number(s): 32.80.Rm

I. INTRODUCTION

Doubly excited valence states imbedded in singly excited Rydberg series are interesting in part because they constitute one of the simplest systems in which the eigenstates are mixtures of ''pure'' states of different configurations. An analogous case which has attracted much attention is a molecule with more than two atoms. Normal vibrational modes are slightly coupled, which allows population to flow back and forth between them, and the advent of short laser pulses has led to the notion of coherently controlling this population flow [1,2], Schumacher and co-workers demonstrated the validity of this notion by observing the population oscillate back and forth between a doubly excited state and degenerate singly excited Rydberg states subsequent to excitation by a short laser pulse [3,4]. They studied the limit in which the characteristic time for the configuration interaction, τ_{CI}, was shorter than τ_K, the Kepler period of the Rydberg electron orbit in the singly excited states. In this limit the doubly excited state interacts significantly with many singly excited Rydberg states, producing eigenstates which are linear superpositions of doubly excited and singly excited states. When they are coherently excited by a short laser pulse a perturbed radial Rydberg wave packet is produced, and it is not particularly surprising that a simple classical description can be developed to describe the subsequent time evolution. Here we complete the picture by considering the opposite limit $\tau_{\mathrm{CI}} \gg \tau_K$. In this case the doubly excited state can only interact appreciably with one singly excited Rydberg state, and then only if the two states and nearly degenerate. Since there is only one Rydberg state involved, it is less obvious that a classical picture is possible, but as we shall show, it is.

Since the states of interest are practically degenerate they behave to some extent like a single Rydberg state. When a Rydberg state is exposed to a laser pulse shorter than τ_K, the pulse removes population near the core, creating a moving hole in the wave function, termed a dark wave packet [5,6], and subsequent photoionization is suppressed when the moving hole is at the ion core [6–10], Quantum mechanically the hole is created by Raman redistribution to nearby states driven by the short, large bandwidth laser pulse. A dark wave packet has been made from a pure Rydberg eigenstate in only one case, and the Raman process proceeded via a lower-lying bound state [11]. In all other cases in which redistribution was observed, the initial eigenstate was a perturbed Rydberg state having some doubly excited character. The difference probably stems from the fact that in a pure Rydberg state there is no clear demarcation between near to and far from the core, while, in a Rydberg state with some doubly excited character, there is a clear distinction between the doubly excited and singly excited parts of the wave function. In general it has been unclear whether the Raman process proceeds via the continuum or bound states. The present work shows that in the case under study the predominant pathway is through a lower lying bound state.

In the sections that follow we briefly outline classical pictures of configuration interaction in the time domain. We describe the experimental procedure for the time domain experiments and present the results for configuration interaction in the time domain and Raman redistribution experiments. Finally, we describe frequency domain measurements which demonstrate that the redistribution occurs by a Raman process through a lower-lying state.

II. CLASSICAL PICTURE OF CONFIGURATION INTERACTION FROM $\tau_{\mathrm{CI}} \gg \tau_K$ TO $\tau_{\mathrm{CI}} \ll \tau_K$

For concreteness we shall discuss the Ba states examined in the work of Schumacher and co-workers [3,4] and in this work. In Fig. 1(a) we show the pure doubly excited $5d7d$ state which is degenerate with the singly excited $6snl$ Rydberg series of the same parity and total angular momentum. Figure 1 also shows that $1/\tau_K$ appears in an energy-level diagram as the separation between the Rydberg states. The pure states of Fig. 1(a) interact, as shown by the double-headed arrow.

When the configuration interaction is taken into account, the eigenstates are in general linear superpositions of the pure doubly excited and singly excited states, and there are two limits, strong and weak configuration interaction, shown in Figs. 1(b) and 1(c). In the case of strong configuration interaction, $\tau_{\mathrm{CI}} \ll \tau_K$, many of the eigenstates have significant $5d7d$ components, as shown in Fig. 1(b). Figure 1(b) also shows that $1/\tau_{\mathrm{CI}}$ appears in the energy-level diagram as

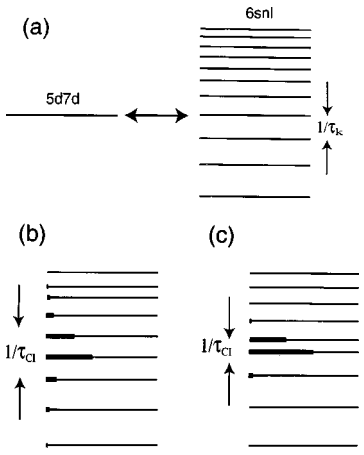

FIG. 1. (a) Energy-level diagram showing the pure $5d7d$ state and the pure $6snl$ Rydberg states. The energy spacing between the Rydberg states is the reciprocal of the Kepler orbital period τ_K. The configuration interaction between the pure states is shown by the double-headed arrow. (b) The mixed eigenstates for strong configuration interaction, $\tau_{CI} \ll \tau_K$, where τ_{CI} is the configuration interaction time. The $5d7d$ state fractions of the mixed eigenstates are shown by bold lines. The pure $5d7d$ state is mixed into many Rydberg states over a bandwidth of $1/\tau_{CI}$. (c) The mixed eigenstates for weak configuration interaction $\tau_{CI} \ll \tau_K$. In this case only two states have appreciable $5d7d$ character.

the width of the band of states containing $5d7d$ character. In the limit of weak configuration interaction, $\tau_{CI} \gg \tau_K$, the $5d7d$ state can only be significantly coupled to a single Rydberg state, and then only if the two pure states are nearly degenerate. This limit is shown in Fig. 1(c).

To develop a classical picture of configuration interaction in the time domain, we consider the case in which the atom is excited to the pure $5d7d$ state at $t=0$ by a short laser pulse. For the case $\tau_{CI} \ll \tau_K$, strong configuration interaction, the initially populated $5d7d$ state ''autoionizes'' into the band of $6snl$ Rydberg states in the time τ_{CI}. The ejected electron departs from the Ba^+ $6s$ ion core but does not have enough energy to escape from the Coulomb potential, and is instead reflected back to the Ba^+ core, returning τ_K later, as shown by Fig. 2(a). The electron then reexcites the core and is itself captured, and the whole process repeats. The probability of finding an atom in the doubly excited $5d7d$ state is a series of spikes τ_{CI} wide separated by τ_K [3,4]. When the atom is in the Rydberg states the electron is radially well localized, so an alternative way of thinking of the atom is as an electron in a classical orbit in which it experiences a time delay as it goes past the ion core [12].

Let us now consider the limit of weak configuration, $\tau_{CI} \gg \tau_K$. Again we assume that at $t=0$ the pure $5d7d$ state is populated. Since τ_{CI} is much longer than τ_K an atom initially in the $5d7d$ state autoionizes into the $6snl$ states over many Kepler periods. Correspondingly, the probability of the Rydberg electron's reexciting the core on any given orbit is small, and once the electron is ejected from the $5d7d$ state it is likely to make many Rydberg orbits before being recaptured, as shown in Fig. 2(b). Since the time constant τ_{CI} for autoionization is much longer than the Kepler time, there is

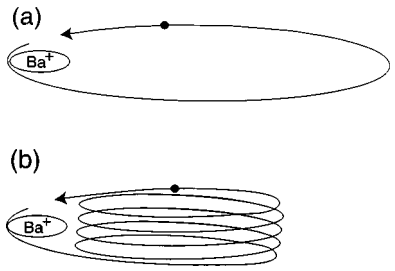

FIG. 2. (a) Classical picture of the electron orbit for strong configuration interaction, $\tau_{CI} \ll \tau_K$. On each orbit the electron is captured and ejected by the Ba^+ core, and suffers a time delay in its orbit. (b) Classical picture of the orbit for weak configuration interaction, $\tau_{CI} \ll \tau_K$. The electron is ejected and recaptured slowly, over many orbits, so the result is minimal spatial localization of the electron's position and only a slow sinusoidal variation in the probability of the electron's being in the Rydberg orbit.

only a sinusoidal oscillation of population in the $5d7d$ state and almost no radial localization of the electron while it is in the Rydberg state. There should only be small moving steps in the radial probability distribution.

In general, describing configuration interaction in the time domain is best done using quantum defect theory (QDT) [13–16], However, the case $\tau_{CI} \gg \tau_K$, in which there are only two levels, is just a two-level quantum beat problem, and all approaches are equally good.

III. EXPERIMENTAL APPROACH

One of our goals is to observe the population oscillate between the pure $5d7d$ state and the singly excited $6sns$ Rydberg series. The approach we have used can be understood with the help of the energy-level diagram of Fig. 3. Ba

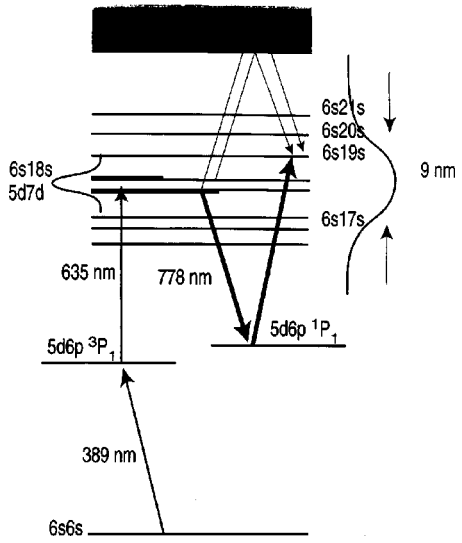

FIG. 3. Energy-level diagram showing the excitation to the perturbed Rydberg states by 389- and 635-nm pulses, and the subsequent removal of population by the 778-nm pulse. The 778-nm pulse both photoionizes the initially populated Rydberg states and redistributes the population to other $6sns$ states by Raman processes through higher- and lower-lying states.

atoms are excited by a 389-nm pulse to the $5d6p\ ^3P_1$ state and then a 0.3-ps, 635-nm pulse to the even-parity $J=0$ eigenstates which lie near term energy 41 450 cm^{-1}. Since the $5d6p\ ^3P_1$ state is not optically connected to the pure $6sns$ Rydberg states, the 635-nm pulse in effect excites the pure $5d7d$ state, which is a coherent superposition of several eigenstates. In Fig. 3 we show the amount of the $5d7d$ character in the eigenstates by the bold lines. As shown in Fig. 3, only two states, the nominal $5d7d$ state and the $6s18s$ state, have appreciable doubly excited character, and we therefore expect to see an approximately sinusoidal oscillation in the population. To observe the population oscillation between the pure $5d7d$ state and the $6sns$ Rydberg states we use a third 100-fs laser pulse, at 778 nm to photoionize the atoms excited by the first two pulses. Light at this wavelength does not photoionize the $6sns$ Rydberg states, but readily photoionizes the $5d7d$ state. Consequently, by observing the photoelectron production as a function of the time delay between the second and third laser pulses, we can monitor the time dependence of the population in the pure $5d7d$ state.

In the experiment Ba atoms effuse from a resistively heated oven, are collimated, and pass between a pair of horizontal field plates 0.46 cm apart, where they are excited by the three laser pulses. All the laser pulses are derived from a titanium:sapphire laser system consisting of a mode-locked oscillator operating at 778 nm and a 1-kHz regenerative amplifier which produces 2-mJ, 100-fs pulses at 778 nm. Half of this light is doubled to produce 389-nm light, and half is used to drive a white light continuum generator and an optical parametric amplifier to produce light at 1.27 μm, which is doubled to 635 nm. The residual 778-nm beam from the doubling passes through a variable delay line. All three beams have diameters of 5 mm before being focused at their crossing with the atomic beam by a 50-cm focal length lens.

The laser beams cross the atomic beam below a hole in the upper field plate. Subsequent to the laser pulses we apply a 6-kV, 1.3-μs rise time pulse to the lower plate. Early in the pulse photoelectrons are expelled through the hole in the upper plate, and later bound Rydberg states are field ionized and expelled at times determined by their binding energies. In either case the resulting electron is detected with a microchannel plate detector above the field plates. With gated integrators we can record either the photoelectron signal or the field ionization signal from a selected Rydberg state or states. These data are stored in a computer for later analysis.

IV. OBSERVATIONS AND COMPARISON TO SIMULATIONS

By delaying the third laser pulse and recording the photoionization signal, we can determine the time dependence of the population in the pure $5d7d$ state. A typical recording of the photoionization signal is shown in Fig. 4(a). While it is plausible that the data represent the expected cosine dependence, the presence of so much background photoionization of the intermediate $5d6p\ ^3P_1$ state by the 778-nm light renders them less than convincing. A better approach is to monitor the population remaining in the $5d7d$ or $6s18s$ states, and in Fig. 4(b) we show the population remaining in the

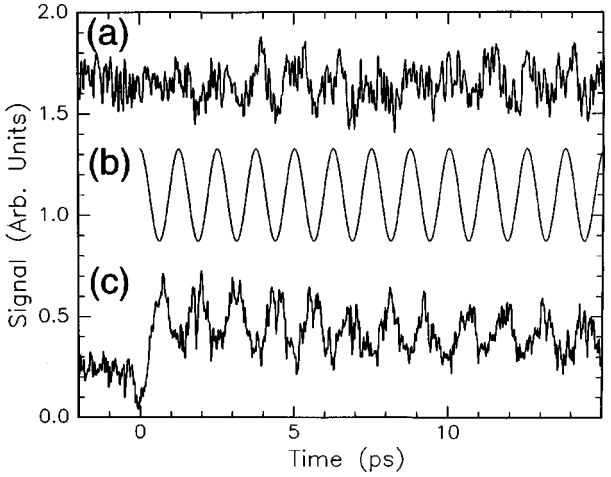

FIG. 4. (a) Photoionization signal, (b) remaining population in the $6s18s$ state, and (c) photoionization signal computed by QDT using known spectroscopic parameters.

$6s18s$ state. The population remaining in the $5d7d$ state exhibits an identical delay time dependence. The signal of Fig. 4(b) clearly shows the expected cosine dependence with a period of 1.25 ps, and it is 180° out of phase with the photoionization signal of Fig. 4(a). The cosine population oscillation of Figs. 4(a) and 4(b) is exactly what one expects for a two-level quantum beat problem, but it is less obvious that the same result will emerge from QDT. Accordingly, we have simulated the observed signal using the method outlined by Lyons *et al.* [14]. Briefly, using QDT we construct wave functions of the form

$$\Psi = a(t)\Psi_{5d7d} + b(t)\Psi_{6s\nu s} \tag{1}$$

for each of the perturbed states using the spectroscopic data [17]. Here ν is the effective quantum number relative to the $Ba^+\ 6s_{1/2}$ limit. We adopt the convention that $a(0)>0$, so $b(0)$ changes sign from below to above the pure $6d7d$ state, in a manner analogous to the π phase shift in a continuum at a resonance. We assume that the second laser pulse at $t=0$ excites a perturbed Rydberg state in proportion to $[a(0)]^2$, its $5d7d$ character, and the intensity of the laser pulse at the state's energy. The initially excited eigenstates are allowed to evolve until time *t*, when the third laser pulse photoionizes the atoms in proportion to $a(t)$ summed over the states excited and squared. In Fig. 4(c) we show the calculated photoionization signal, which is also a cosine with a 1.25-ps period. This simple result is a consequence of only two states having significant $5d7d$ character. The calculated signal is in phase with the photoionization signal and 180° out of phase with the signal from the population remaining in the $6s18s$ state.

Due to the weakness of the configuration interaction in this case, the second laser excites principally two states, which are quite closely spaced, 26.6 cm^{-1}, and the third laser has a short enough pulse width that it redistributes the population over other Rydberg states, which we detect by state-selective field ionization. As shown in Fig. 5, when time-dependent field ionization traces are taken with and without

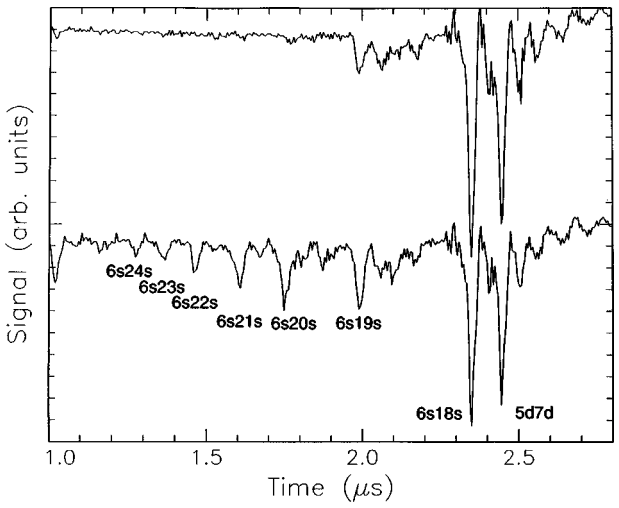

FIG. 5. Time-resolved field ionization traces obtained (a) without and (b) with the 778-nm laser. In the former the higher-lying $6sns$ $n>18$ states are not apparent, but they are quite evident in the latter.

the third pulse, the redistribution produced by the third pulse is quite evident. We expected to see a 1.25-ps oscillation in the signal from any of the $6sns$, $n\neq 18$ states, corresponding to the 26.6-cm^{-1} separation of the states predominantly excited. However, we saw oscillations at other frequencies as well. Figure 6 shows recordings of the field ionization signal from the $6sns$ states as a function of time delay between the second and third laser pulses. It is clear from Fig. 6 that there are oscillations with periods other than 1.25 ps. In Fig. 7 we show the Fourier transforms of the data of Fig. 6. By comparing the observed features to the known intervals, given in Table I, it is apparent that prominent features are observed at the frequencies corresponding to the interval between the $5d7d$ state and the state under observation.

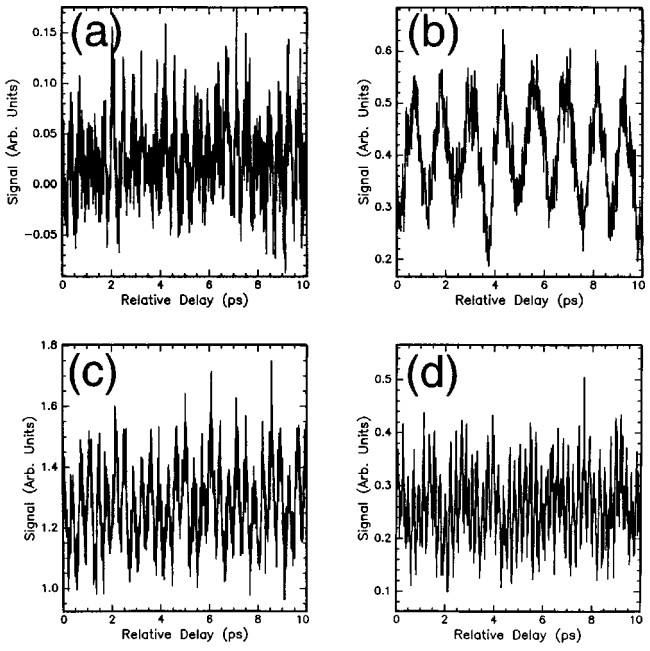

FIG. 6. Field ionization signals from (a) $6s17s$, (b) $6s18s$, (c) $6s19s$, and (d) $6s20s$ states vs time delay between the 635- and 778-nm laser pulses. Only in (b) is the expected 1.25-ps beat period apparent. In the other frames higher frequencies obscure it.

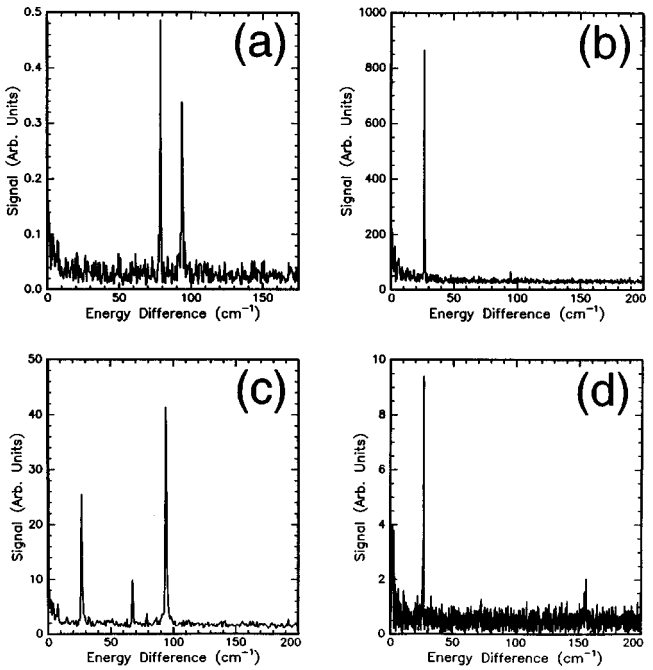

FIG. 7. Fourier transforms of the data of (a) $6s17s$, (b) $6s18s$, (c) $6s19s$, and (d) $6s20s$. In all but (b) frequencies other than 26.6 cm^{-1} are visible. All but one of these frequencies correspond to the intervals between the state being observed and the $5d7d$ state, as listed in Table I.

The high-frequency oscillations in the populations of states other than the $5d7d$ and $6s18s$ states arise from the fact that they are populated via two interfering pathways. The first pathway is direct excitation by the second laser. The second laser pulse produces a wave packet of Rydberg eigenstates which are excited with amplitudes in proportion to the square roots of their perturber character, as shown in Fig. 3. Thus, the $6s17s$ and $6s19s$ states, which have $\sim$1% perturber character, are excited with $\sim$15% of the amplitudes of the $6s18s$ and $5d7d$ states. If the optical pulse saturates the transition, the relative amplitudes of states other than the $6s18s$ and $5d7d$ states are enhanced. The second pathway is excitation by the second laser to the $5d7d$ state followed by a Raman transition to the $6sns$ states of $n\neq 18$ driven by the

TABLE I. $5d7d$-$6sns$ and $6s18s$-$6sns$ intervals.

Interval	Frequency (cm^{-1})
$5d7d$-$6s17s$	78.8
$5d7d$-$6s18s$	26.6
$5d7d$-$6s19s$	94.1
$5d7d$-$6s20s$	154.1
$6s18s$-$6s17s$	105.4
$6s18s$-$6s19s$	67.5
$6s18s$-$6s20s$	127.5

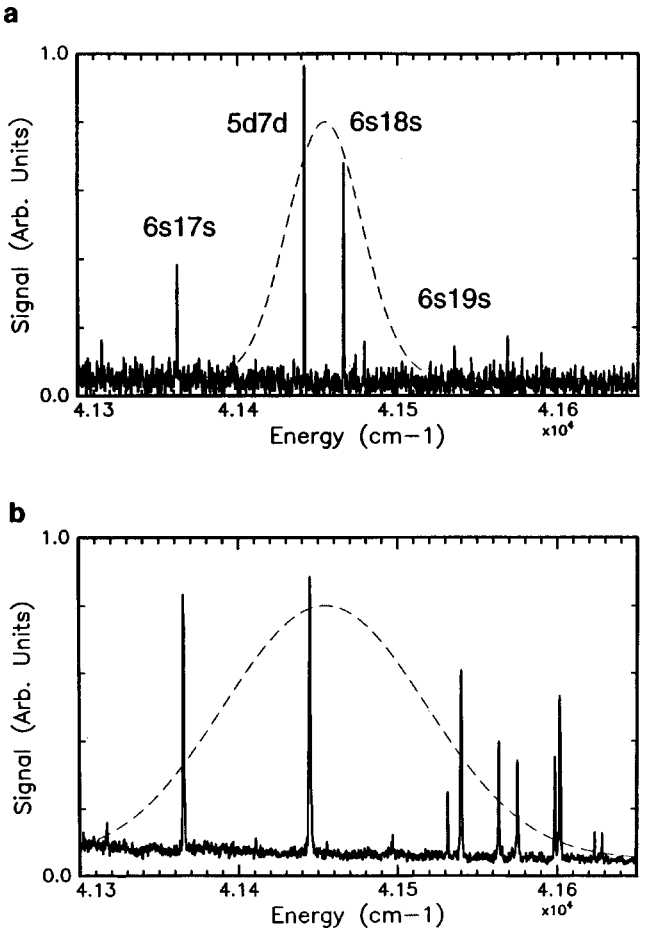

FIG. 8. (a) Excitation spectra with 5-ns-long dye laser pulses (a) from the $5d6p\ ^1P_1$ state, and (b) from the $5d6p\ ^3P_1$ state. In (a) and (b) the bandwidths of the 635- and 778-nm lasers in the time domain experiment, respectively, are shown by broken lines. In (a) it is apparent that primarily the $5d7d$ and $6s18s$ states are excited by the 635-nm laser. In (b) the $6s18s$ state is conspicuously absent, and Raman redistribution via the $5d6p\ ^3P_1$ state cannot occur from the initially populated $6s18s$ state.

third laser. Varying the time delay between the second and third lasers leads to the observed interference oscillations.

Following the above line of reasoning we would expect to see both the $5d7d$-$6sns$ and $6s18s$-$6sns$ frequencies, not just the former, but the Raman redistribution evidently occurs from only the $5d7d$ state, not from the $6s18s$ state. Since we see a 26.6-cm^{-1} oscillation in the photoionization signal, it is apparent that both the $6s18s$ and $5d7d$ states are well coupled to the continuum, which suggests that the Raman redistribution probably occurs via a lower-lying intermediate state. In fact, the $5d6p\ ^1P_1$ state lies one 778-nm photon below the $5d7d$ and $6s18s$ states, and is a reasonable candidate for the intermediate state. To explain the observed redistribution it would have to be optically connected to the $5d7d$ state but not the $6s18s$ state.

We had initially assumed, based on the observations of Ref. [18], that any low-lying $5d6p$ state would be optically connected to the $5d7d$ states but not to the $6sns$ Rydberg states. However, the redistribution data remind us that this assumption is not always valid. To clarify both the excitation by the second laser and the redistribution, we have recorded the frequency domain excitation spectra from both the $5d6p\ ^3P_1$ and $5d6p\ ^1P_1$ states to the region around 41 450 cm^{-1}. Briefly, we used one 5-ns dye laser at 389 (350) nm to prepare the $5d6p\ ^3P_1\ (^1P_1)$ state and a second dye laser near 635 (776) nm to reach the $J=0$ states near 41 450 cm^{-1}. To detect the Rydberg atoms we used a third laser at 455 nm to excite atoms in the $6sns$ states to the autoionizing $6p_{3/2}ns$ states. Since it is possible to saturate the last transition by orders of magnitude, it provides a detection efficiency of one. Scanning the wavelength of the second laser while detecting the ions resulting from autoionization gives us the desired excitation spectra. In Fig. 8(a) we show the spectrum obtained from the $5d6p\ ^3P_1$ state. As we had initially assumed, there are two strong transitions, to the $5d7d$ and $6s18s$ states.

Using the $5d6p\ ^1P_1$ state as an intermediate state, we observed the spectrum of Fig. 8(b), in which we observe the $5d7d$ state and all the $6sns$ states but $6s18s$. The spectrum of Fig. 8(b) is exactly what is required to explain our Raman redistribution data, i.e. there is a Raman coupling via $5d6p\ ^1P_1$ state to the $6sns\ n\neq 18$ states from the $5d7d$ state, but not from the $6s18s$ state. As a consequence, we are confident that in this case the Raman redistribution occurs entirely through the bound states. The reason it does not pass through the continuum is probably as follows. The coupling of both the $5d7d$ and $6s18s$ states to the continuum is strong, due to their high perturber content, but the coupling of the continuum to $6sns\ n\neq 18$ states is weak, since they are pure Rydberg states.

V. CONCLUSION

These data and those of Schumacher and co-workers [3,4] span the range from $\tau_{CI}\gg\tau_K$ to $\tau_{CI}\ll\tau_K$. We have shown that, over the entire range, the time dependence of the configuration interaction can be quantitatively represented using QDT and that simple classical pictures can be developed. In addition, we have clearly shown that Raman redistribution occurs by way of a lower-lying state, not through the continuum.

ACKNOWLEDGMENTS

It is a pleasure to acknowledge useful discussions with R. R. Jones and the support of the National Science Foundation.

[1] J. J. Gerdy, M. Dantus, R. M. Bowman, and A. H. Zewail, Chem. Phys. Lett. **171**, 1 (1990); B. Kohler, V. V. Yakovlev, J. Che, J. L. Krause, M. Messina, K. R. Wilson, N. Schwentner, R. M. Whitnell, and Y. J. Yan, Phys. Rev. Lett. **74**, 3360 (1995).

[2] D. J. Tannor and S. A. Rice, J. Chem. Phys. **83**, 5013 (1985).

[3] D. W. Schumacher, B. J. Lyons, and T. F. Gallagher, Phys. Rev. Lett. **78**, 4359 (1997).

[4] D. W. Schumacher, D. I. Duncan, R. R. Jones, and T. F. Gallagher, J. Phys. B **29**, L397 (1996).
[5] H. Stapelfeldt, D. G. Papaioannou, L. D. Noordam, and T. F. Gallagher, Phys. Rev. Lett. **67**, 3223 (1991).
[6] R. R. Jones and P. H. Bucksbaum, Phys. Rev. Lett. **67**, 3215 (1991).
[7] K. Burnett, P. L. Knight, B. R. M. Piraux, and V. C. Reed, Phys. Rev. Lett. **66**, 301 (1991).
[8] L. D. Noordam, H. Stapelfeldt, D. I. Duncan, and T. F. Gallagher, Phys. Rev. Lett. **68**, 1496 (1992).
[9] J. H. Hoogenraad, Phys. Rev. A **50**, 4133 (1994).
[10] B. Piraux, E. Huens, and P. Knight, Phys. Rev. A **44**, 721 (1991).
[11] R. R. Jones, C. S. Raman, D. W. Schumacher, and P. H. Bucksbaum, Phys. Rev. Lett. **71**, 2575 (1993).
[12] F. T. Smith, Phys. Rev. **118**, 349 (1960).
[13] W. A. Henle, H. Ritsch, and P. Zoller, Phys. Rev. A **36**, 683 (1987).
[14] B. J. Lyons, D. W. Schumacher, D. I. Duncan, R. R. Jones, and T. F. Gallagher, Phys. Rev. A **57**, 3712 (1998).
[15] F. Texier and Ch. Jungen, Phys. Rev. Lett. **81**, 4329 (1998).
[16] S. T. Cornett, H. R. Sadeghpour, and M. J. Cavagnero, Phys. Rev. Lett. **82**, 2488 (1999).
[17] M. Aymar, P. Camus, M. Dieulin, and C. Morillon, Phys. Rev. A **18**, 2173 (1978).
[18] O. C. Mullins, Y. Zhu, and T. F. Gallagher, Phys. Rev. A **32**, 243 (1985).